Research Article

Journal of Innate Immunity

J Innate Immun
DOI: 10.1159/000504322

Received: March 26, 2019
Accepted: October 16, 2019
Published online: December 4, 2019

Rapamycin Treatment Reduces Acute Myocarditis Induced by *Trypanosoma cruzi* Infection

Thabata L.A. Duque[a, b] Cynthia M. Cascabulho[b] Gabriel M. Oliveira[a]
Andrea Henriques-Pons[b] Rubem F.S. Menna-Barreto[a]

[a]Laboratório de Biologia Celular, Instituto Oswaldo Cruz, Rio de Janeiro, Brazil; [b]Laboratório de Inovações em Terapias, Ensino e Bioprodutos, Instituto Oswaldo Cruz, Rio de Janeiro, Brazil

Keywords
Trypanosoma cruzi · Chagas disease · Autophagy · Rapamycin · Acute infection

Abstract
Chagas disease affects millions of people mainly in Latin America and is a protozoan illness caused by the parasite *Trypanosoma cruzi*. Chagasic cardiomyopathy is the leading cause of mortality of infected patients, due to compromised electrical and mechanical cardiac function induced by tissue remodeling, especially fibrosis, and lymphocytic infiltration. Some cellular biochemical pathways can be protective to the heart, and we tested if the in vivo activation of the autophagic machinery by rapamycin could reduce parasite-induced myocarditis. Regarding the expression of LC3, an autophagy marker, we observed its upregulation in the cardiac tissue of infected untreated mice. However, after rapamycin treatment, an autophagy inducer, infected mice showed reduced electrical cardiac dysfunctions, myocarditis, cardiac damage, and reduced production of pro-inflammatory cytokines by the heart. On the other hand, the parasite's life cycle was not affected, and we observed no modulations in cardiac tissue or blood parasitemia. Our data indicate that, at least partially, autophagy induction controls inflammation in the heart¸ illustrating the complexity of the pathways that concur to the development of the infection.

Introduction

Chagas disease is a neglected illness caused by the protozoan parasite *Trypanosoma cruzi*. It was described in 1909 by the Brazilian physician Carlos Chagas and affects millions of people worldwide, especially in Latin America. One of the most important clinical manifestations is chagasic cardiomyopathy, which is observed in acute and chronic symptomatic patients [1]. In about 30% of the chronic patients, electrocardiographic (ECG) abnormalities, such as arrhythmias and atrioventricular blockade; lymphoid inflammatory infiltration, fibrosis, cardiac damage are observed [2, 3].

Cellular inflammatory foci are mostly composed of $CD8^+$ T lymphocytes after parasite infection in different host cell types; however, macrophages and other myeloid cells are also presented [4]. The infection triggers several

KARGER

E-Mail karger@karger.com
www.karger.com/jin

Dr. Rubem F.S. Menna-Barreto
Laboratório de Biologia Celular, Instituto Oswaldo Cruz
Fiocruz, Av. Brasil 4365
Manguinhos 21040-360 (Brazil)
E-Mail rubemsadok@gmail.com

biochemical pathways, including autophagy, which is involved in cytoplasmic components recycling and other intracellular functions. It has also been described as a pathway that controls *T. cruzi*-host cell interplay [5]. Autophagy is indispensable for cell survival, leading to cellular structures and organelles turnover and is upregulated by stress situations such as nutrient depletion, hormone deprivation, or cytokine induction. Uncontrolled or imbalanced autophagy leads to autophagic death or other programmed cell death, as apoptosis and necroptosis [6, 7]. Macroautophagy (hereafter referred as autophagy) is regulated by proteins named Atg, which are responsible for the initiation, nucleation, elongation, and closure of vesicles (autophagosomes) that contain the structures targeted to lysosomal degradation. One of these proteins is LC3 (microtubule-associated protein light chain3), also named Atg 8, a required component that recruits phosphatidylethanolamine to autophagosomes [8].

Another key molecule for many biological functions, including autophagy, is the mammalian target of rapamycin (mTOR), it is found gathered with different proteins composing the complexes 1 (mTORC1) and 2 (mTORC2). Although the function of mTORC1 is also associated with lipids and proteins biosynthesis, autophagy induction through the inactivation of mTOR is the main effect of the complex, especially after rapamycin treatment. This drug is a classical autophagic inducer and a clinically used immunosuppressive drug that impairs lymphocyte proliferation [9, 10] and reduces organ rejection in cardiac and renal-transplanted patients [11], for example. Several mTORC1 blockers are available for patients' treatments, but this therapeutic alternative must be carefully planned [12], as primary biological pathways can be affected directly or indirectly, as the reduction of inflammatory responses and cell death. In the case of experimental models using rapamycin, it leads to increased longevity and can improve cardiac function in different pathologies [13]. For cardiac treatment, it was shown that the induction of autophagy is beneficial after ischemic events but deleterious in reperfusion [14]. These results illustrate the complexity of mTOR-dependent pathways and the broad implication of autophagy induction.

Regarding trypanosomatid infections, few results have revealed autophagic proteins involved in in vivo [15–17]. Moreover, the role played by autophagy, especially LC3, in the heart of in vivo *T. cruzi* infected mice is unknown. In acutely *T. cruzi* infected-mice, the ratio of LC3-II/I is increased and p62, an adaptor protein of autophagosomes, is further upregulated in infected mice fed with high-fat diet [17]. Rapamycin treatment in the context of *T. cruzi* infection has only been demonstrated in vitro, showing decreased parasite proliferation [18]. In *Leishmania major*, in vivo treatment using rapamycin reduced cutaneous inflammatory lesions in mice [16].

In this study, we evaluated rapamycin-dependent modulations of mTORC1, focusing on the autophagy importance over in vivo *T. cruzi* infection. Parasite infection upregulated the autophagy marker LC3 in cardiac cells in the acute phase. Moreover, when infected mice were treated with rapamycin, there were no alterations in circulating or cardiac parasitemia, but the inflammatory response and cardiac function were downmodulated. Rapamycin treatment preserved electric cardiac function, reduced cardiac damage, myocarditis, and the levels of tissue pro-inflammatory cytokines interferon (IFN)-γ, tumor necrosis factor (TNF), and interleukin (IL)-6. These results add new insights to the field, approaching central and controversial aspects of the rapamycin treatment in *T. cruzi* infection.

Materials and Methods

Ethics Statement

The use of mice and experimental procedures are in accordance with Brazilian Law 11.794/2008 and regulations of the National Council of Animal Experimentation Control. Mice were housed for at least 1 week before experimentation at the Divisão de Experimentação Animal at the Laboratório de Inovações em Terapias, Ensino e Bioprodutos – Instituto Oswaldo Cruz, FIOCRUZ under conditions complying with the "Guide for the Care and Use of Laboratory Animals" (DHEW Publication No. [NIH] 80–23, revised 1985). Animals were housed at 4 individuals per cage, at 20–24 °C under cycles of 12 h light and 12 h dark, and provided sterilized water and rodent chow ad libitum. All experimental procedures performed were reviewed and approved by Fiocruz Committee of Ethics in Animal Research (LW16/13), according to the resolution 196/96 of the National Health Council of Brazilian Ministry of Health.

Mice, Infection, and Treatment with Rapamycin

Five-week-old male Swiss Webster outbred mice were obtained from animal facilities of ICTB/FIOCRUZ (Institute of Science and Biomodels Technology/Fiocruz) and Biotério Central (UNICAMP/ Brazil). Mice were intraperitoneally (i.p.) infected with 1×10^3 blood trypomastigotes forms of *T. cruzi* Y strain in 200 μL of PBS. After 5 days of infection, parasitemia was daily quantified using the Pizzi-Brener method [19] until 15 days post-infection (dpi); thereafter, it was weekly scored until 30 dpi (when blood parasitemia is subpatent). The rapamycin treatment (1 mg/kg/day daily i.p. for 10 days; LC Labs, Woburn, USA) started on 5 dpi. The drug was diluted in dimethylsulfoxide (Merck, Darmstadt, Germany), never exceeding 1% of the final solution. Control animals received i.p. injection of vehicle solution [20].

Biochemical Analysis

Individual blood was collected after tail tip excision on 0, 8, and 15 dpi, and cardiac puncture was done only on 15 dpi. Renal function was evaluated based on urea and creatinine and hepatic and cardiac damage were assessed using alanine aminotransferase and aspartate aminotransferase and creatine kinase isotype MB respectively. We used commercially available kits according to the manufacturer's recommendations (Doles, Goiânia, Brazil).

ECG Analysis

ECG recordings and analysis were performed in control uninfected and *T. cruzi*-infected mice obtained in physically restrained (non-sedated).All mice were fixed in the supine position, and 8-lead ECGs were recorded using an 18-gauge needle as electrodes subcutaneously implanted in each limb, and 2 similar electrodes at precordial positions lead II. The ECG traces were registered using a standard lead (dipolar lead DII), acquired with the amplitude set to give 2 mV/1s. ECGs were registered by using a band-pass filter (Bio Amp – AD Instruments, Sydney, Australia) between 0.1 and 100 Hz. Amplification and analog-digital conversion were conducted with a Powerlab 16S instrument (AD Instruments) and digital recordings (16 bit, 4 kHz/channel) were analyzed using the Scope (version 3.6.10) software. To quantify the signal-averaged ECG, the mouse signal-averaged ECG extension (version 1.2) program and a template-matching algorithm were used. ECG parameters were analyzed using the following standard criteria: (i) variation at *p* wave and PR, QRS and QT intervals measured in ms, (ii) the heart rate monitored by beats/minute (bpm) for cardiac arrhythmias [21]. The relation between the QT and RR intervals was individually assessed to obtain physiologically relevant values for the heart rate-corrected QT interval (QTc) through Bazzet's formula [22].

Cardiac and Spleen Cells Isolation and Phenotypic Analysis

On 15 dpi, spleen and heart were collected for phenotypic analysis. For cardiac analysis, ventricles were cut in fragments of around 2 mm thick in ice-cold PBS. Then, they were submitted to a mechanical and enzymatic dissociation in a solution of 100 U/mL collagenase type 2 (Worthington, Lakewood, USA) and submitted to 5 cycles of enzymatic digestion under gentle agitation for 15 min at 37 °C [23]. The cells were centrifuged at 4 °C 150 × *g* for 10 min, filtered using 40 μm-mesh cell strainers (Falcon Thermo, Waltham, USA), and transferred to ice-cold DMEM medium supplemented with 10% FBS and 3 mM calcium chloride. For splenic analysis, splenocytes were obtained after red blood cell lysis by hypoosmotic buffer using PBS and distilled water for 10 s. For autophagic evaluation ex vivo, splenocytes were incubated with 100 μM of leupeptin (Sigma, St Louis, USA) in DMEM supplemented with 10% FBS for 1 h at 37 °C [24].

For phenotypic labeling, splenocytes and cardiac inflammatory cells were incubated in DMEM medium supplemented with 10% FBS and 10% inactivated normal sheep serum to block FcγR and subsequently incubated for 30 min at 4 °C with previously titrated antibodies: CD127, CD3, CD4, CD8, CD62L, CD44 (Biolegend, San Diego, EUA). For cell death analysis, the samples were incubated with Live/Dead Far-Red fixable dead cell (Thermo) in PBS for 30 min at room temperature. After cell surface labeling, intracellular labeling was performed using Cytofix/Cytoperm Kit (BD, Franklin Lakes, USA), according to manufacturer's instructions, followed by incubation of 30 min with anti-LC3B and anti-rabbit AlexaFluor 488 antibodies at 4 °C, and washed twice with Perm/Wash Buffer (BD). The acquisition was performed in a FACS Aria Ilu II (BD) and data analysis in FlowJo X (LLC, BD).

Cytokines Analysis

On 15 dpi, plasma and heart cytokines were evaluated by flow cytometry. Plasma was obtained by cardiac puncture using heparin and cardiac fragments were incubated in ice-cold extraction buffer with protease cocktail inhibitor (Roche, Basel, Switzerland). All samples were then centrifuged at 500 × *g* and supernatants were used for cytokine analysis. TNF, IL-6, IL-10, IL-17, IFN-γ, and IL-2 were measured using the cytometric-bead array Th1 Th2 Th17 kit (BD), according to manufacturer's recommendation. The samples were acquired using a FACS Calibur (BD), and data analysis was performed using the FCAP software (BD). Protein concentration was determined by bicinchoninic acid kit (Pierce, Thermo), following the manufacturer's recommendations.

Histopathological Analysis

On 15 dpi, the hearts were also collected for histopathological analysis. The ventricles were collected, embedded in OCT (Sakura, Torrance, USA), and frozen at liquid nitrogen and stored at –80 °C. Five micrometre-thick cardiac sections were done using a cryostat and fixed in a 4% paraformaldehyde solution for 10 min at room temperature. For histopathological analysis, the slices were stained using hematoxylin and eosin and at least 20 fields per sample were evaluated using Image J (HIH) for cellular inflammatory infiltration and amastigotes nests. For LC3 puncta evaluation, the incubation with primary antibody (final concentration: 10 μg/mL; Sigma Aldrich) was performed overnight at 4 °C in permeabilization and blocking buffer (PBS supplemented with 5% FBS, 10% inactivated sheep serum, 0.5% Triton X-100, 0.1% tween 80, and 2% bovine serum albumin). Then, all samples were incubated for 1 h with secondary antibody (anti-rabbit Alexa Fluor 488 [final concentration: 1.3 μg/mL; Invitrogen]). Cell nucleus was labeled using 4′, 6-diamidino-2-phenylindole (final concentration: 0.2 μg/mL; Sigma Aldrich) and Evans blue (Sigma Aldrich) was used for counterstaining.

Statistical Analysis

Data are expressed as arithmetic means ± SEM. All statistical tests were performed using Mann-Whitney *t* test, ANOVA and other appropriate post-tests were used to examine the statistical significance in GraphPad Prism (version 6.0). The differences were considered statistically significant when $p \leq 0.05$.

Results

Autophagy Is Upregulated during Chagasic Cardiomyopathy in Vivo

First, we evaluated if autophagy in cardiac fibers is upregulated in vivo after *T. cruzi infection*, as observed in the liver [17, 25], and in vitro in different lineage cells by others [26, 28, 29]. To this end, the mice were infected and the presence of LC3 puncta was investigated by immunostaining in cardiac ventricles sections (Fig. 1). LC3

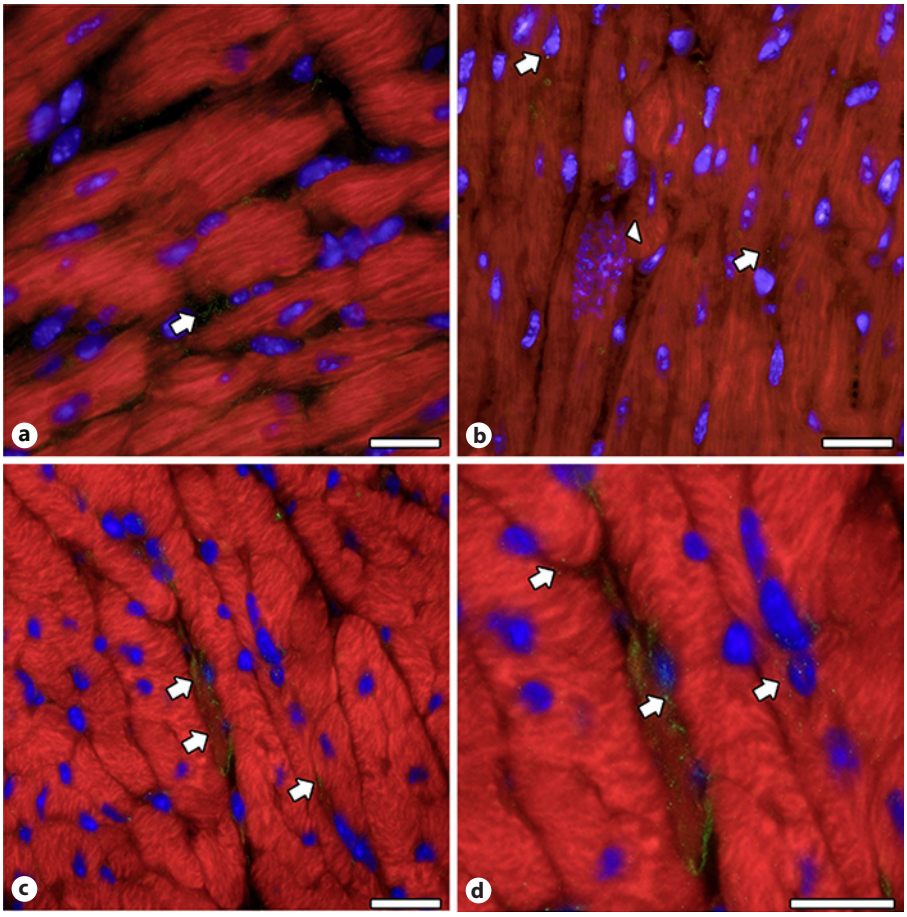

Fig. 1. Autophagy induction in cardiac tissue infected with *T. cruzi* in vivo. **a–d** Representative panel of immunofluorescence of LC3 (green) counterstained with Evans blue (red) from cardiac tissue from uninfected (**a**) and infected 15 dpi (**b–d**). Note that LC3 (white arrows) is not associated with the parasite nest (**b**, white arrowhead) but in cardiomyocytes (**c**, **d**). **d** Inset highlights LC3 puncta inside cardiac cell. Bars: 20 μm.

puncta were rarely detected in uninfected mice in our analysis (Fig. 1a). Although LC3 puncta were not present associated with amastigote nests in the cardiac fibers (Fig. 1b), LC3 puncta were observed distributed in the heart and endomysial cells surrounding cardiac fibers (Fig. 1c, d).

Rapamycin Does not Modulate Parasitemia Parameters However Protects Cardiac Function during T. cruzi Infection in Vivo

We then investigated whether autophagy induction by rapamycin in infected mice would affect the course of the infection. Rapamycin is an FDA-approved drug that induces autophagy and can be used in heart-transplanted patients, improving cardiac function. We observed that the treatment with rapamycin prevented animal mortality after the infection (online suppl. Fig. S1A; see www.karger.com/doi/10.1159/000504322 for all online suppl. material), although not affecting circulating parasitemia (online suppl. Fig. S1B). There were no differences between all groups of mice until 8 dpi, nevertheless, on 15 dpi both groups of infected mice (treated and untreated) showed reduced body weight when compared with both groups of uninfected mice (online suppl. Fig. S1C). The levels of hepatic aspartate aminotransferase and alanine aminotransferase enzymes did not change during the time-period evaluated in any of the groups tested (online suppl. Fig. S2A, B). Regarding renal function, on 8 dpi, we observed higher levels of urea (online suppl. Fig. S2C) and creatinine (online suppl. Fig. S2D) only in the untreated infected group, and both markers decreased to control levels on 15 dpi. This result suggested that rapamycin treatment protected the renal function after infection (online suppl. Fig. S2A–D). Normalized heart weight was increased only in the untreated infected group (online suppl. Fig. S3A) and both groups of infected mice showed increased relative spleen weight (splenomegaly; online suppl. Fig. S3B) and liver weight (online suppl. Fig. S3C) when compared with control mice. However, in rapamycin-treated infected mice, we observed reduced spleno-

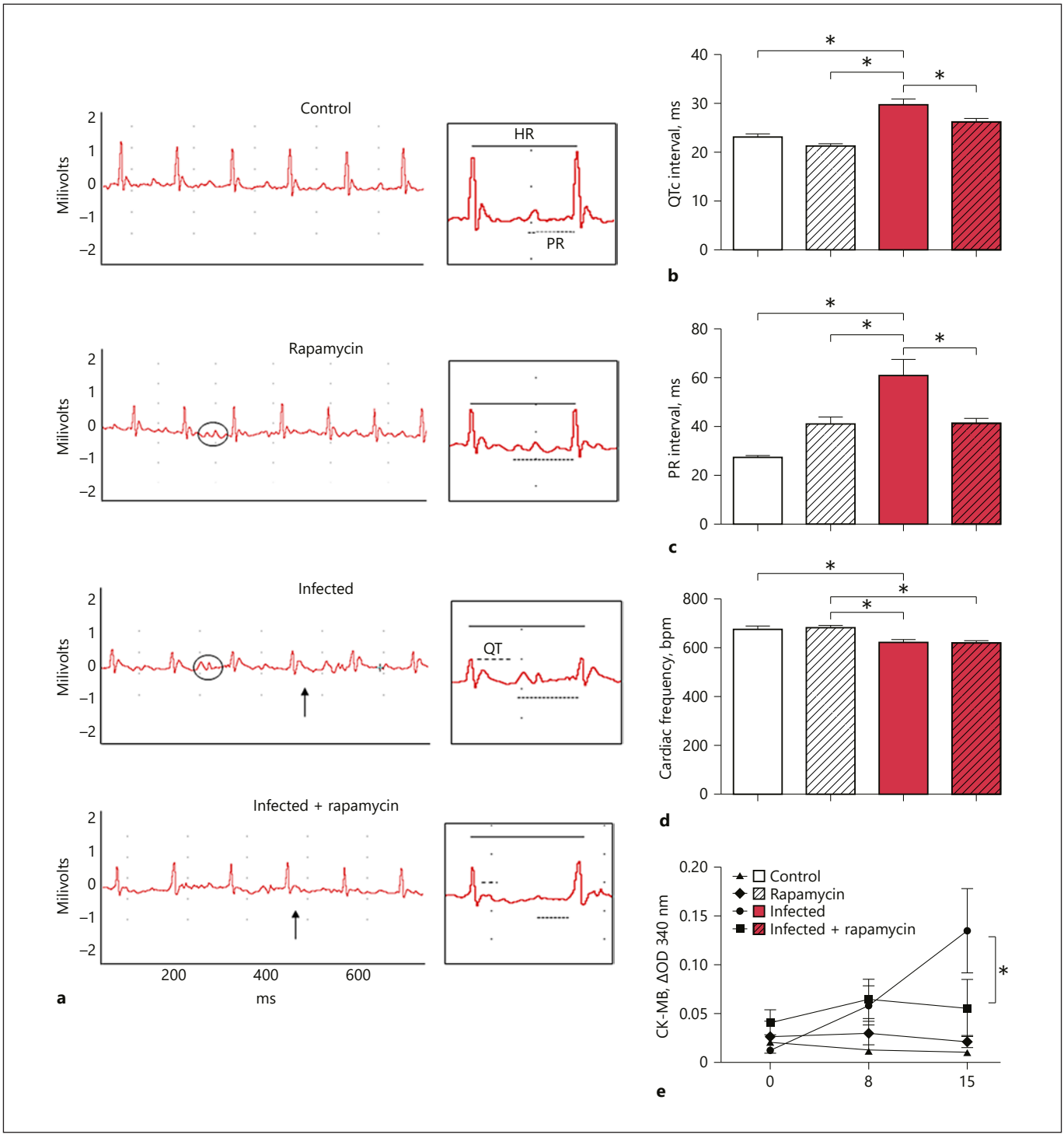

Fig. 2. Rapamycin protects cardiac function during acute *T. cruzi* infection in vivo. (**a**) Representative panel of ECG traces. QTc interval (**b**), PR interval (**c**) and cardiac frequency (**d**) from 15 dpi. CK-MB (**e**) was also evaluated weekly ($n = 3$, mean of 4 animals per group, in triplicate). Asterisks indicate significant differences ($p < 0.05$, Two-way ANOVA and Bonferroni post test). CK-MB, creatine kinase isotype MB.

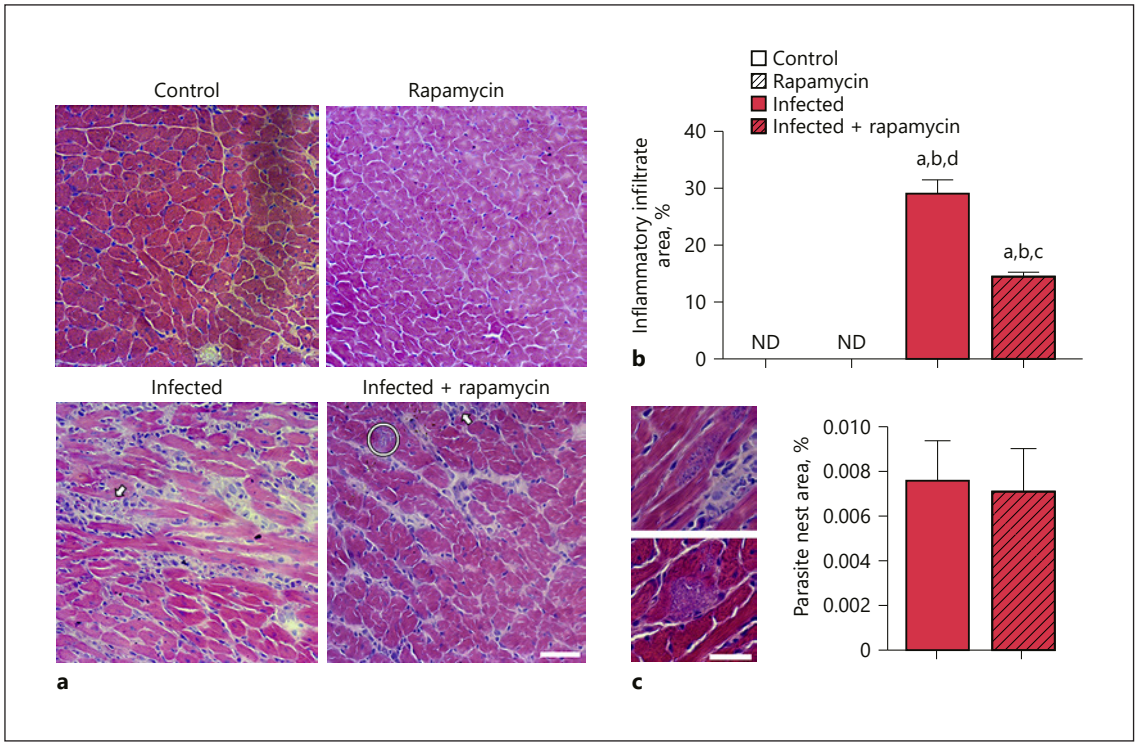

Fig. 3. Rapamycin reduces infiltrate inflammatory in *T. cruzi* infection in vivo. **a** Representative panels from HE staining of heart in 15 dpi. Bars: 50 μm. **b** Infiltrate inflammatory area – with at least 10 inflammatory cells (%) and (**c**) parasite nest area (%) from infected (upper panel) and infected + rapamycin (bottom panel; n = 3, mean 4 animals per group, in triplicate). Bars: 20 μm. $^{a-d}$ Indicate significant differences in relation to control, rapamycin, infected and infected + rapamycin, respectively ($p < 0.05$, Two-way ANOVA and Bonferroni post test). ND, not determined.

megaly when compared to infected and untreated mice (online suppl. Fig. S3B). The infection induced thymus atrophy in both groups of infected mice, although more pronounced atrophy was observed after rapamycin treatment (online suppl. Fig. S3D).

In *T. cruzi* infection, there are alterations in the cardiac electrical conduction system in both acute and chronic symptomatic patients. Most electrical disturbs registered by ECG in the murine model are an atrioventricular blockage, identified by irregular and increased QTc intervals and cardiac arrhythmias, as sinus bradycardia [21]. The analysis of ECG traces (Fig. 2a) in infected mice revealed that at least 50% of the animals had atrioventricular blockage (data not shown). Moreover, infected untreated animals showed increased QTc and PR (Fig. 2b, c) intervals when compared with control mice, and the treatment led to a significant decrease in both parameters, indicating a protective cardiac role of rapamycin. The PR interval was affected in rapamycin-treated uninfected animals, with an increase of about 1.5-fold when compared with untreated and uninfected mice (Fig. 2c; average ± SD in the Control: 27.2 ± 0.7; Rapamycin: 41.0 ± 3.1; Infected: 60.9 ± 6.8; Infected + Rapamycin: 41.2 ± 2.3; Fig. 2c). Considering cardiac frequency (Fig. 2d), we observed bradycardia in about 25% of infected mice (data not shown), which was not affected in uninfected rapamycin treated-mice. The evaluation of creatine kinase isotype MB confirmed the cardiac damage induced by the infection on 15 dpi, and there was a reduction in the enzyme activity after rapamycin treatment (Fig. 2e).

It is known that cardiac damage is induced by both the intracellular parasite infection and the host immune response [27]. During the acute infection, inflammatory foci and amastigote nests are diffusely distributed in the heart. In our model, the infection led to an intense migration of mononuclear cells to the heart, as expected, and the treatment with rapamycin significantly reduced the local inflammatory response (Fig. 3a, b), although not leading to control levels. The analysis of parasite nests in the cardiac ventricles (Fig. 3c), showed no differences when comparing both groups of infected mice (Fig. 3c).

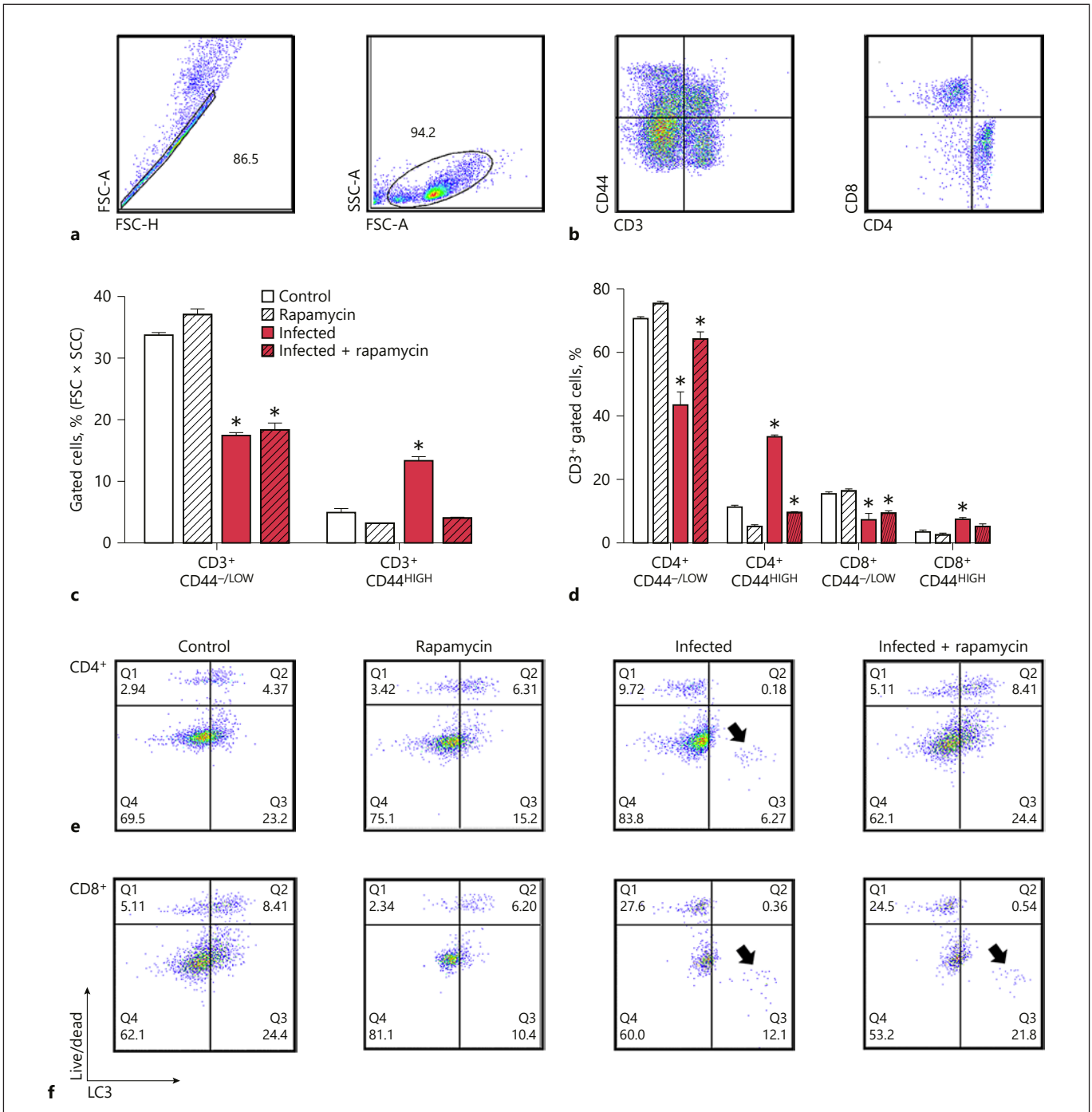

Fig. 4. Rapamycin decreases activation in T cells from spleen during *T. cruzi* infection in vivo. a, b Flow cytometry gating strategy for identifying T lymphocytes from the spleen. Representative panel was chosen from an infected group. **a** Doublets were excluded using FSC-A × FSC-H and after cell size (SSC-A × FSC-A) right panel. **b** Cells were first identified as $CD3^+$ (left panel, also demonstrating CD44 strategy) and after by CD4 × CD8 (right panel). **c** Percentage (in cell size gate) of $CD3^+$ $CD44^{-/low}$ and $CD3^+CD44^{high}$ from each group and (**d**) in $CD3^+$ gated cells the percentage of $CD4^+$ $CD44^{-/low}$ and $CD4^+CD44^{high}$ and $CD8^+$ $CD44^{-/low}$ and $CD8^+CD44^{high}$. Bars represent mean ± SEM. **e**, **f** Cells were labeled with LC3 and Live/Dead to evaluate autophagy and cell death, respectively, in $CD4^+$ (**e**) and $CD8^+$ (**f**) gated cells. Numbers inside each gate represent the percentage of events. All experiments were performed in a pool of 4 hearts each group in 15 dpi, triplicate. Asterisks indicate significant differences in relation to control and rapamycin uninfected group ($p < 0.05$, two-way ANOVA and Bonferroni post test).

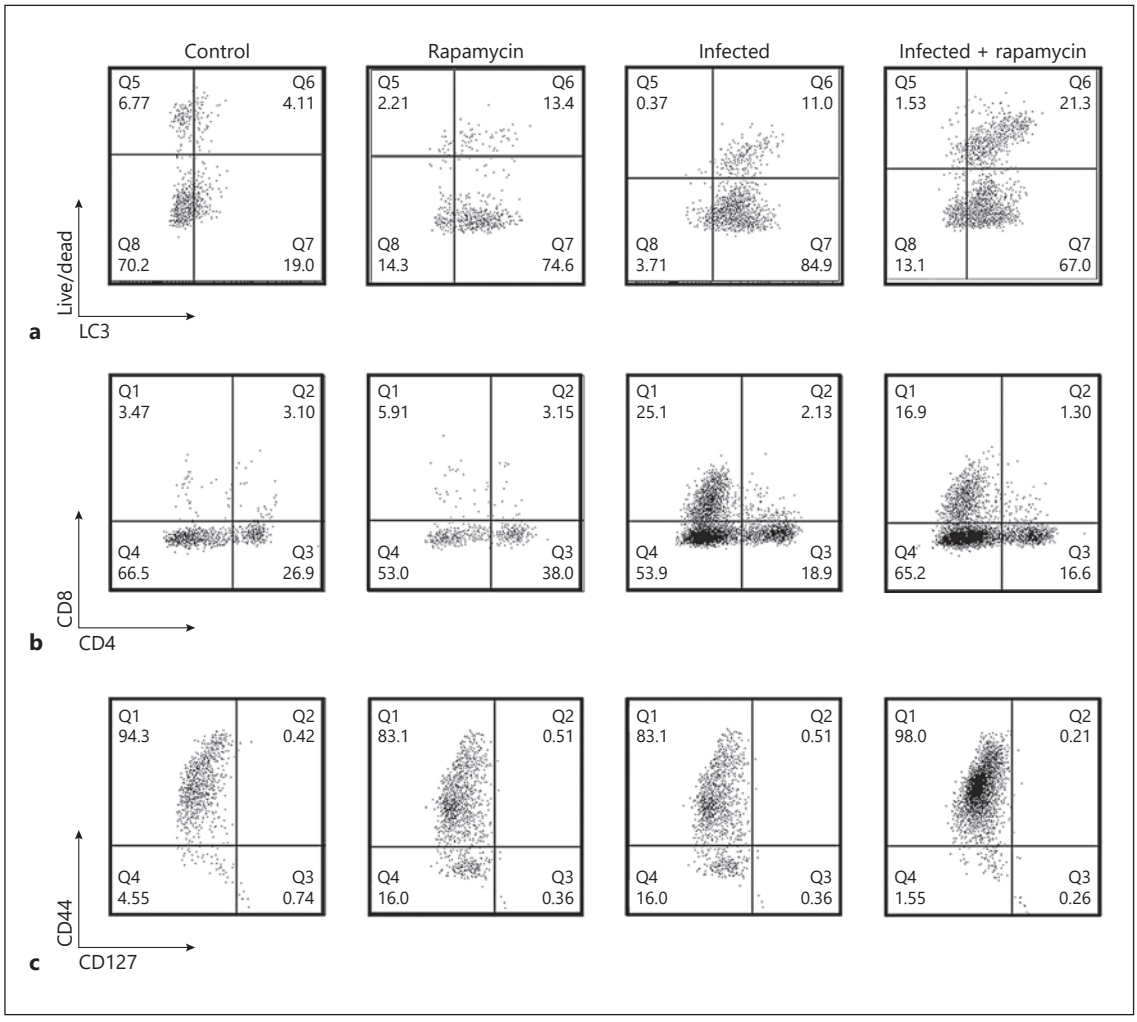

Fig. 5. Rapamycin does not modulate T-cell activation in heart in acute *T. cruzi* infection in vivo and infection induces autophagy (**a–c**) T cells were identified after doublet exclusion, cell size and $CD3^+CD62L$- and labeled with LC3 and Live/Dead (**a**), CD4 and CD8 (**b**) and CD44 and CD127 (**c**). In (**a**), $CD3^+$ gated cells were evaluated LC3 expression and cell death, (**b**) phenotypic and (**c**) activation. The numbers inside each gate represent the percentage of events. All experiments were performed in a pool of 4 hearts for each group in 15 dpi.

Rapamycin Increases Autophagy in the Spleen But Not in Cardiac T-Cell Population in Infected Animals

As rapamycin-treated mice showed reduced splenomegaly after infection, we decided to analyze T-cells activation and autophagy cell death in splenocytes. The analysis was done in the morphological gate of lymphocytes after doublet exclusion and in the gate of $CD3^+$ events (Fig. 4a, b). In the spleen, CD4 and CD8 T cells were analyzed as antigen-unstimulated cells ($CD44^{-/low}$) or as effector/effector memory T cells ($CD44^{high}$; Fig. 4c) and we found few differences in the percentage of CD4 regarding Infected group (Control: 54.2 ± 2.8; Rapamycin: 50.5 ± 4.0; Infected: 68.6 ± 5.8; Infected+ Rapamycin: 61.7 ± 7.1) and in CD8 T cells in rapamycin uninfected-mice (Control: 15.2 ± 5.2; Rapamycin: 24.7 ± 1.9; Infected: 16.9 ± 0.7; Infected + Rapamycin: 15.0 ± 1.1). We observed no differences between the groups when comparing double negative and double-positive cells (data not shown). The infection increased the percentage of $CD3^+CD44^{high}$ cells (Fig. 4c), which was not detected in the other groups. In contrast, infection decreased $CD3^+CD44^{low}$ cells (Fig. 4c). When we discriminate $CD3^+$ gated cells in CD4 and CD8, we noted that an increase of $CD44^{high}$ population is due to CD4 T cells (Fig. 4d). When we discerned splenocytes from effector memory T cells based on CD127 labeling, we observed 25.15% of effector ($CD44^{high}$ $CD127^{-/low}$) and

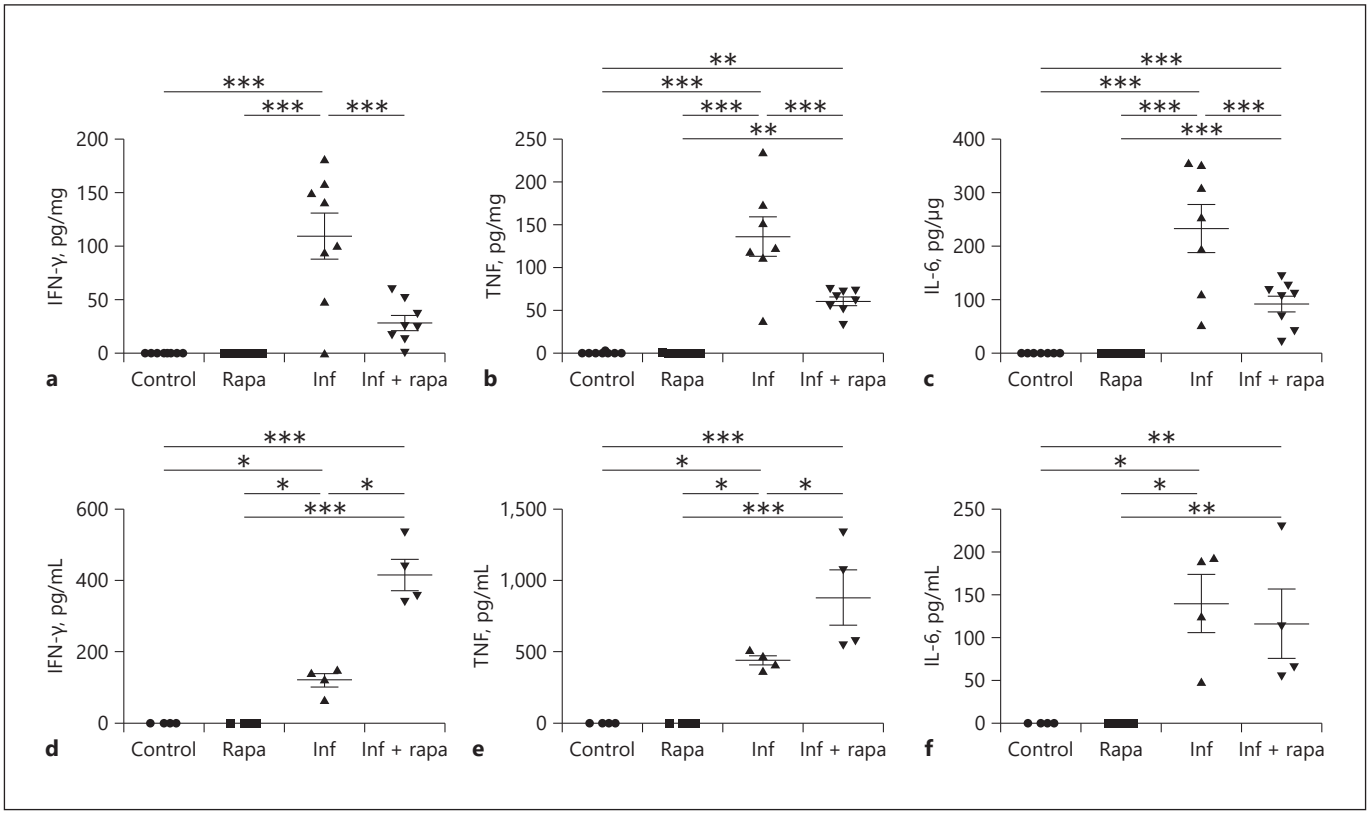

Fig. 6. Rapamycin reduces inflammatory cytokines in *T. cruzi* – infected heart but not in the serum. Cytokine production from cardiac ventricle from control, rapamycin, infected and infected-rapamycin animals in dpi 15. **a** IFN-γ, (**b**) TNF and (**c**) IL-6. Data are expressed in pg of cytokine per mg of total protein. Plasma cytokines were evaluated in dpi 15. **d** IFN-γ, (**e**) TNF and (**f**) IL-6 (at least 4 animals per group). Asterisks indicate significant differences (* $p < 0.05$, ** $p < 0.01$, *** $p < 0.001$, two-way ANOVA and Bonferroni post test).

17.3% of effector memory T cells ($CD44^{high}$ $CD127^{high}$) after the infection. On the other hand, in the rapamycin-infected group, effector T cells were drastically reduced to 0.3% of $CD3^+$ cells, and there were no modulations in effector memory T cells that were 16.3% (data not shown). The analysis of cell death and LC3 labeling in CD4 and CD8 T cells showed that LC3 was upregulated in a subpopulation after the infection (Fig. 4e, f, arrow). Moreover, only in rapamycin-treated infected mice, we observed that $CD4^+$ T cells are more susceptible to autophagy cell death ($LC3^+$, $Live/Dead^+$) than $CD8^+$ T cells (Fig. 4e, f). As flow cytometry assay with LC3 labeling does not allow us to observe conjugation to phosphatidylethanolamine (usually in microscopy as LC3 puncta), we decided to incubate the splenocytes with leupeptin [24] to evaluate LC3 without molecule degradation by lysosomes. We observed that indeed ex vivo leupeptin incubation further evidenced the LC3 labeling in infected and rapamycin-treated infected groups (online suppl. Fig. S4).

As splenic T-cell populations were regulated by rapamycin treatment, we evaluated if cardiac inflammatory foci, especially CD8 T cells [4], were also modulated. Thus, cardiac T cells were harvested from all groups and evaluated by flow cytometry. First, the percentage of gated $CD3^+$ cardiac T cell in infected groups are almost threefold more than uninfected groups (uninfected groups: 6.5% ± 3.4 versus infected groups: 22.5% ± 5.6, in gated cells). When compared with control mice, all other groups showed an increase in $LC3^+$ cells, either Live/Dead positive or negative events in $CD3^+$ gated cells (Fig. 5a), confirming our hypothesis of autophagic upregulation during infection. Regarding CD4 and CD8 T cells in cardiac tissue, as expected, $CD8^+$ cells were further increased in *T. cruzi*-infected animals (Fig. 5b) and both $CD4^+$ and $CD8^+$ populations were vastly $CD44^{+/high}$ $CD127^-$ T cells (Fig. 5c), a phenotype compatible with effector T cells.

Proinflammatory Cytokines Decrease in Rapamycin-Treated Chagasic Heart

Once no significant differences could be detected in effector cardiac T cells regarding rapamycin treatment during infection, we investigated heart and plasma cytokines from untreated and rapamycin-treated animals. In the heart of infected mice, proinflammatory cytokines IFN-γ, TNF, and IL-6 were increased, and we observed a reduction of all these molecules after rapamycin treatment (Fig. 6a–c). In the plasma, IFN-γ and TNF were at higher levels in the rapamycin-treated infected mice, when compared with untreated infected mice (Fig. 6d, e) and no differences were detected in IL-6 levels after infection (Fig. 6f). We also evaluated IL-17, IL-10, IL-4, and IL-2 and these cytokines were not detected in plasma or heart tissue (data not shown).

Discussion

Host autophagy machinery is crucial for cellular pathways in immune responses, including lymphocyte activation and intracellular parasite infections, as previously demonstrated [16]. In the case of in vitro *T. cruzi* infection, some reports described the association of pathogen control with host autophagy and mTORC1 pathway [18, 26, 28, 29], even with some conflicting results. In this work, we evaluated the upregulation of autophagy in *T. cruzi* infection in vivo and autophagy upmodulation/mTORC1 inhibition by rapamycin as a mechanism of controlling inflammation and cardiac damage triggered by the parasite.

Here, we demonstrated that acute murine infection induces LC3 upregulation in the cardiac tissue. On 15 dpi, the myocardium is already reorganizing cells due to inflammatory infiltration, likewise initiating endothelial and microvascular cells migration. In vitro studies indicate that *T. cruzi* infects microvascular and endothelial cells [30, 31], and in early infection (before circulating parasitemia can be detected), amastigote forms are present in coronary microvascular cells [30]. We believe that on 15 dpi, the prominent LC3 labeling in the infected heart is due to cardiac reorganization. This is also observed in other cardiomyopathies, that autophagy is upregulated in connective tissue, organizing cardiac remodeling [32, 33]. Besides, the evaluation of autophagy in splenocytes and cardiac T cells corroborates the higher activation of this process in T cells from infected mice, also in effector $CD44^{high}$ T cells, which implies that in vivo infection is also an autophagy inducer, as recently shown by immunoblotting using the liver of infected animals [17, 25]. As described in in vitro studies, the pathogen can induce autophagy, upregulating LC3 and other autophagy genes. Indeed, few studies describe how mechanisms underlie this activation, and we believe that in our model, the parasite triggers host cell adaptations because of cell damage, which could induce autophagy, including mTOR pathway.

The upregulation of autophagy observed in infected cardiac tissue and immune cells from secondary target tissues, like the spleen, prompted us to evaluate if autophagy modulation, particularly the mTOR pathway, could impair parasite damage in mammalian host cells. As rapamycin and other autophagy inducers as a starvation medium have shown to control infection in vitro [18], we evaluated whether rapamycin also had a protective role in vivo. Rapamycin inhibits especially mTORC1, by interacting with FKBP12 [34] and is already used in heart transplant, promoting cardioprotection [35, 36]. The immunomodulatory effects of this mTORC1 blocker, which upregulates autophagy and is currently used in in vivo studies [10, 11, 16, 20] prompted us to evaluate rapamycin as a potentially beneficial drug to the host immune response in acute *T. cruzi* infection. Other mTOR inhibitors as Torin 1 and 2 and pp242 are also autophagy inducers, but modulate the mTOR complex through different mechanisms: they seem to inhibit both mTORC1 and mTORC2 more efficiently than rapamycin [37, 38], but LC3 expression in cells showed a different regulation between inhibitors [39]. Besides, Torin 1 and pp242 have not been evaluated in heart and in immune response, while rapamycin was demonstrated as having advantageous effects [32, 35, 40].

Rapamycin did not decrease parasite load, but instead, it protects the host, acting in (i) autophagy upregulation in spleen and heart (ii) reduction of splenomegaly, (iii) cardiac protection by decreased inflammation and electrical disturbances. During rapamycin treatment of infected mice, the maintenance of effector memory T cells was similar to what is observed in lymphocytic choriomeningitis vaccination [40] and heterologous prime-boost vaccine in *T. cruzi* chronic infection [41]. Interestingly, rapamycin and other immunosuppressors enhance vaccine efficacy as inducers of memory T cells [42], promoting protective immunity. Our results reinforce the hypothesis of protective mechanisms mediated by rapamycin during infection in a lymphoid target organ. In cardiac T cells, we could not detect these effects because T cells had recently migrated to the target organ. It is possible that with the progression of the infection, memory T cells (especially central memory T cells) could also be

observed [41], and rapamycin could upregulate this population in the heart.

We observed in the heart, remarkable effects in cardioprotection such as decreased inflammation and reduction in the electrical cardiac conduction system. PR and QTc intervals disturbance were also present in clinical drugs treatment for Chagas disease as some antiarrhythmic drugs as verapamil and amiodarone may also affect negatively the heart function [2, 43]. One of our most unexpected and intriguing results was the downmodulation of cytokine in the heart, revealing inflammation downregulation. In CD8 T cells, proteomic analysis already revealed that rapamycin reduced protein content, including proinflammatory cytokines [44]. This could partially explain the reduction of proinflammatory cytokines in the heart. Furthermore, a nutritionally poor environment could downregulate IFN-γ mRNA in T cells [45], which is also observed in our experiment, reinforcing this hypothesis. However, it is worth mentioning that mTORC1 could limit proinflammatory cytokine through NF- kB activation [46], which might suggest that in plasma, rapamycin treatment blocked mTORC1 and increased IFN-γ and TNF, are probably released from other organs.

The controversial results of proinflammatory cytokines also demonstrate that other deleterious effects could not improve immune response and fail to control the infectious disease. Here we used rapamycin to evaluate how autophagy induction could modulate host response, especially the immune mechanisms, against a parasite that in acute infection increased inflammation in the heart.

Regarding these results, rapamycin-induced autophagy controls inflammation in the heart and spleen in vivo reducing damage in acute murine infection. Moreover, the molecular mechanism of rapamycin function in the infection must be further investigated in the future, considering inflammation and electric cardiac conduction.

Acknowledgments

The authors are grateful to Daniela Beghini, Juliana Guimarães, Natalia Vacani, Pedro Paulo Manso, Marcos Meuser and Patrícia Bernardino for their excellent technical support. We also thank Mariana Gandini for cytometer acquisition and writing suggestions and Flow Cytometry and Transmission Electron Microscopy Facilities from Oswaldo Cruz Institute and Fiocruz (RPT08A). The present work was supported by grants from Fundação Carlos Chagas Filho de Amparo à Pesquisa do Estado do Rio de Janeiro, Coordenação de Aperfeiçoamento de Pessoal de Nível Superior, Conselho Nacional de Desenvolvimento Científico e Tecnológico and Papes/Fundação Oswaldo Cruz (Fiocruz).

Disclosure Statement

The authors declare no commercial or financial conflict of interest.

Author Contributions

T.L.A.D.: performed all assays. C.M.C.: performed in vivo experiments and cytokines analysis. G.M.O.: performed ECG analysis. A.H.-P. and T.L.A.D.: performed flow cytometry analysis. R.F.S.M.-B. and A.H.-P.: contributed to the design and supervision of the experiments. T.L.A.D., A.H.-P., and R.F.S.M.-B.: wrote the manuscript. All authors have read and approved the final manuscript.

References

1 Tanowitz HB, Machado FS, Spray DC, Friedman JM, Weiss OS, Lora JN, et al. Developments in the management of Chagas cardiomyopathy. Expert Rev Cardiovasc Ther. 2015 Dec;13(12):1393–409.

2 Machado FS, Jelicks LA, Kirchhoff LV, Shirani J, Nagajyothi F, Mukherjee S, et al. Chagas heart disease: report on recent developments. Cardiol Rev. 2012 Mar-Apr;20(2):53–65.

3 Bestetti RB, Muccillo G. Clinical course of Chagas' heart disease: a comparison with dilated cardiomyopathy. Int J Cardiol. 1997 Jul; 60(2):187–93.

4 Henriques-Pons A, Oliveira GM, Paiva MM, Correa AF, Batista MM, Bisaggio RC, et al. Evidence for a perforin-mediated mechanism controlling cardiac inflammation in Trypanosoma cruzi infection. Int J Exp Pathol. 2002 Apr;83(2):67–79.

5 Kaur J, Debnath J. Autophagy at the crossroads of catabolism and anabolism. Nat Rev Mol Cell Biol. 2015 Aug;16(8):461–72.

6 Klionsky DJ. Autophagy: from phenomenology to molecular understanding in less than a decade. Nat Rev Mol Cell Biol. 2007 Nov; 8(11):931–7.

7 Kroemer G, Levine B. Autophagic cell death: the story of a misnomer. Nat Rev Mol Cell Biol. 2008 Dec;9(12):1004–10.

8 Yang Z, Klionsky DJ. Mammalian autophagy: core molecular machinery and signaling regulation. Curr Opin Cell Biol. 2010 Apr;22(2): 124–31.

9 Dumont FJ, Su Q. Mechanism of action of the immunosuppressant rapamycin. Life Sci. 1996;58(5):373–95.

10 Ballou LM, Lin RZ. Rapamycin and mTOR kinase inhibitors. J Chem Biol. 2008 Nov;1(1-4):27–36.

11 Khan S, Salloum F, Das A, Xi L, Vetrovec GW, Kukreja RC. Rapamycin confers preconditioning-like protection against ischemia-reperfusion injury in isolated mouse heart and cardiomyocytes. J Mol Cell Cardiol. 2006 Aug;41(2):256–64.

12 Gottlieb RA, Pourpirali S. Lost in translation: miRNAs and mRNAs in ischemic preconditioning and ischemia/reperfusion injury. J Mol Cell Cardiol. 2016 Jun;95:70–7.

13 Deretic V, Levine B. Autophagy, immunity, and microbial adaptations. Cell Host Microbe. 2009 Jun;5(6):527–49.

14 Huang C, Yitzhaki S, Perry CN, Liu W, Giricz Z, Mentzer RM Jr, et al. Autophagy induced by ischemic preconditioning is essential for cardioprotection. J Cardiovasc Transl Res. 2010 Aug;3(4):365–73.

15 Cyrino LT, Araújo AP, Joazeiro PP, Vicente CP, Giorgio S. In vivo and in vitro Leishmania amazonensis infection induces autophagy in macrophages. Tissue Cell. 2012 Dec;44(6):401–8.
16 Franco LH, Fleuri AK, Pellison NC, Quirino GF, Horta CV, de Carvalho RV, et al. Autophagy downstream of endosomal Toll-like receptor signaling in macrophages is a key mechanism for resistance to Leishmania major infection. J Biol Chem. 2017 Aug;292(32):13087–96.
17 Lizardo K, Almonte V, Law C, Aiyyappan JP, Cui MH, Nagajyothi JF. Diet regulates liver autophagy differentially in murine acute Trypanosoma cruzi infection. Parasitol Res. 2017 Feb;116(2):711–23.
18 Rojas Márquez JD, Ana Y, Baigorrí RE, Stempin CC, Cerban FM. Mammalian Target of Rapamycin Inhibition in Trypanosoma cruzi-Infected Macrophages Leads to an Intracellular Profile That Is Detrimental for Infection. Front Immunol. 2018 Feb;9:313.
19 Brener Z. Therapeutic activity and criterion of cure on mice experimentally infected with Trypanosoma cruzi. Rev Inst Med Trop Sao Paulo. 1962 Nov-Dec;4:389–96.
20 Kimball SR, Jefferson LS, Nguyen HV, Suryawan A, Bush JA, Davis TA. Feeding stimulates protein synthesis in muscle and liver of neonatal pigs through an mTOR-dependent process. Am J Physiol Endocrinol Metab. 2000 Nov;279(5):E1080–7.
21 Campos JD, Hoppe LY, Duque TL, de Castro SL, Oliveira GM. Use of Noninvasive Parameters to Evaluate Swiss Webster Mice During Trypanosoma cruzi Experimental Acute Infection. J Parasitol. 2016 Apr;102(2):280–5.
22 Mitchell GF, Jeron A, Koren G. Measurement of heart rate and Q-T interval in the conscious mouse. Am J Physiol. 1998 Mar;274(3):H747–51.
23 Cascabulho CM, Bani Corrêa C, Cotta-de-Almeida V, Henriques-Pons A. Defective T-lymphocyte migration to muscles in dystrophin-deficient mice. Am J Pathol. 2012 Aug;181(2):593–604.
24 Pietrocola F, Demont Y, Castoldi F, Enot D, Durand S, Semeraro M, et al. Metabolic effects of fasting on human and mouse blood in vivo. Autophagy. 2017 Mar;13(3):567–78.
25 Casassa AF, Vanrell MC, Colombo MI, Gottlieb RA, Romano PS. Autophagy plays a protective role against Trypanosoma cruzi infection in mice. Virulence. 2019 Dec;10(1):151–65.
26 Romano PS, Arboit MA, Vázquez CL, Colombo MI. The autophagic pathway is a key component in the lysosomal dependent entry of Trypanosoma cruzi into the host cell. Autophagy. 2009 Jan;5(1):6–18.
27 Cruz JS, Machado FS, Ropert C, Roman-Campos D. Molecular mechanisms of cardiac electromechanical remodeling during Chagas disease: role of TNF and TGF-β. Trends Cardiovasc Med. 2017 Feb;27(2):81–91.
28 Martins RM, Alves RM, Macedo S, Yoshida N. Starvation and rapamycin differentially regulate host cell lysosome exocytosis and invasion by Trypanosoma cruzi metacyclic forms. Cell Microbiol. 2011 Jul;13(7):943–54.
29 Onizuka Y, Takahashi C, Uematsu A, Shinjo S, Seto E, Nakajima-Shimada J. Inhibition of autolysosome formation in host autophagy by Trypanosoma cruzi infection. Acta Trop. 2017 Jun;170:57–62.
30 Hassan GS, Mukherjee S, Nagajyothi F, Weiss LM, Petkova SB, de Almeida CJ, et al. Trypanosoma cruzi infection induces proliferation of vascular smooth muscle cells. Infect Immun. 2006 Jan;74(1):152–9.
31 Factor SM, Cho S, Wittner M, Tanowitz H. Abnormalities of the coronary microcirculation in acute murine Chagas' disease. Am J Trop Med Hyg. 1985 Mar;34(2):246–53.
32 Nishida K, Kyoi S, Yamaguchi O, Sadoshima J, Otsu K. The role of autophagy in the heart. Cell Death Differ. 2009 Jan;16(1):31–8.
33 Deroyer C, Magne J, Moonen M, Le Goff C, Dupont L, Hulin A, et al. New biomarkers for primary mitral regurgitation. Clin Proteomics. 2015 Sep;12(1):25.
34 Laplante M, Sabatini DM. An emerging role of mTOR in lipid biosynthesis. Curr Biol. 2009 Dec;19(22):R1046–52.
35 Shioi T, McMullen JR, Tarnavski O, Converso K, Sherwood MC, Manning WJ, et al. Rapamycin attenuates load-induced cardiac hypertrophy in mice. Circulation. 2003 Apr;107(12):1664–70.
36 Wang ZV, Ferdous A, Hill JA. Cardiomyocyte autophagy: metabolic profit and loss. Heart Fail Rev. 2013 Sep;18(5):585–94.
37 Feldman ME, Apsel B, Uotila A, Loewith R, Knight ZA, Ruggero D, et al.: Active-Site Inhibitors of mTOR Target Rapamycin-Resistant Outputs of mTORC1 and mTORC2. PLoS Biol. 2009 Feb;7(2):e38.
38 Leontieva OV, Blagosklonny MV: Gerosuppression by pan-mTOR inhibitors. Aging (Albany NY). 2016 Dec;8(12):3535–51.
39 Xu S, Li L, Li M, Zhang M, Ju M, Chen X, et al. Impact on Autophagy and Ultraviolet B Induced Responses of Treatment with the MTOR Inhibitors Rapamycin, Everolimus, Torin 1, and pp242 in Human Keratinocytes. Oxid Med Cell Longev. 2017;2017:5930639.
40 Araki K, Turner AP, Shaffer VO, Gangappa S, Keller SA, Bachmann MF, et al. mTOR regulates memory CD8 T-cell differentiation. Nature. 2009 Jul;460(7251):108–12.
41 Vasconcelos JR, Dominguez MR, Neves RL, Ersching J, Araújo A, Santos LI, et al. Adenovirus vector-induced CD8 T effector memory cell differentiation and recirculation, but not proliferation, are important for protective immunity against experimental Trypanosoma cruzi Infection. Hum Gene Ther. 2014 Apr;25(4):350–63.
42 Nam JH. Rapamycin: could it enhance vaccine efficacy? Expert Rev Vaccines. 2009 Nov;8(11):1535–9.
43 Nada A, Gintant GA, Kleiman R, Gutstein DE, Gottfridsson C, Michelson EL, et al. The evaluation and management of drug effects on cardiac conduction (PR and QRS intervals) in clinical development. Am Heart J. 2013 Apr;165(4):489–500.
44 Hukelmann JL, Anderson KE, Sinclair LV, Grzes KM, Murillo AB, Hawkins PT, et al. The cytotoxic T cell proteome and its shaping by the kinase mTOR. Nat Immunol. 2016 Jan;17(1):104–12.
45 Blagih J, Coulombe F, Vincent EE, Dupuy F, Galicia-Vázquez G, Yurchenko E, et al. The energy sensor AMPK regulates T cell metabolic adaptation and effector responses in vivo. Immunity. 2015 Jan;42(1):41–54.
46 Weichhart T, Costantino G, Poglitsch M, Rosner M, Zeyda M, Stuhlmeier KM, et al. The TSC-mTOR signaling pathway regulates the innate inflammatory response. Immunity. 2008 Oct;29(4):565–77.